GEOLOGICA BELGICA (2000) 3/1-2 : 67 - 86

SEISMIC HAZARD ASSESSMENT IN BELGIUM

Didier LEYNAUD[1], Denis JONGMANS[1], Hervé TEERLYNCK[1] & Thierry CAMELBEECK[2]

(12 figures & 2 tables)

1. Laboratory of Engineering Geology and Applied Geophysics, Liège University, Bat. B19, 4000 Liège.
2. Royal Observatory of Belgium, Avenue Circulaire, 3, 1180 Bruxelles.

ABSTRACT. The seismic hazard assessment has been conducted on the Belgian territory conforming to Eurocode 8, the European earthquake building code. The study was performed using the seismological database of the Royal Observatory of Belgium and the publications and open reports available for geological and geophysical data. The seismic hazard in Belgium was evaluated with a probabilistic analysis, using the public software SEISRISK III from the U.S. Geological Survey. The output consists of hazard maps showing the distribution of the horizontal peak ground acceleration for a return period of 475 years. Different maps are presented according to the choices that can be made on the attenuation laws and the definition of the seismic source zones. The computations have been made assuming that all Belgian territory is constituted by rock, as requested by Eurocode 8.

KEYWORDS: seismic hazard, probabilistic assessment, peak ground acceleration, Eurocode 8, Belgium.

1. Introduction

During the last 16 years, Belgium has experienced two damaging earthquakes in 1983 (Liège, Ms=4.7) and in 1992 (Roermond, Ms=5.4). The Liège earthquake, which strongly affected some suburbs of the town, showed that the seismic risk needs to be evaluated in heavily populated areas where the known seismic activity is low to moderate. This event had a significant impact on the development of the Belgian seismic network and initiated numerous research activities in the different fields of earthquake engineering (among others, Camelbeeck & De Becker, 1985, Camelbeeck, 1990 and 1994, Jongmans & Campillo, 1990, Jongmans, 1991). Good quality instrumental data allowed to bring a new insight in the seismotectonics of Belgium (Camelbeeck, 1990). On another hand, historical earthquakes have been re-evaluated and the seismic catalogue has been dramatically improved (e.g., Ambraseys, 1985, Alexandre, 1994, Alexandre, personal communication). Recently, paleoseismological investigations have been initiated in the Roer Valley graben with the aim of identifying large past earthquakes and characterising the fault activity on a longer time period (Camelbeeck & Meghraoui, 1998). These studies provide reliable information on the long-term seismicity between the Lower Rhine embayement and the North Sea.

Since the pioneering work of Zaczek and Van Gils (1978), the seismic hazard in Belgium has not been re-assessed for the whole territory of Belgium. In the present paper, a seismic hazard map has been computed for Belgium within the frame of the Eurocode 8 (Commission of the European Communities, 1993). EC8 is the document defining the common European rules for the design and the construction of civil engineering structures in seismic areas. In order to apply it, each national authority is in charge of assessing the seismic hazard and subdividing its territory in seismic zones. Each zone is characterised by a ground acceleration (on the rock) for a return period of 475 years. On this basis, the seismic actions in EC8 are defined as response spectra which also vary with the local soil conditions.

The seismic hazard assessment is the first part of the risk estimation process. The definition of the terms and the general methodology used in probabilistic seismic hazard are given in appendix 1. The main four steps to obtain a seismic hazard map are (1) the definition of seismic source zones from instrumental and historical earthquake data, as well as from geological and geophysical information, (2) the evaluation of the seismic activity for each zone, (3) the definition of attenuation laws and (4) the computation of the seismic hazard map using the public software SEISRISK III (Bender and Perkins, 1987).

As the return period for large earthquakes is very long in an intra-plate area like Belgium, the available seismological data are necessarily incomplete and affected by uncertainty. At each step, some decisions have to be made, which may strongly influence the final results. Geological and geophysical data (mainly gravity and aeromagnetic maps) have also been used for the definition of seismic sources. The spirit of this study is to be as transparent as possible

in a way that anybody could check our results. With this aim, we only used public data and software and we tried to clearly specify and discuss our choices.

2. Geological and geophysical setting

2.1. Geological setting

The geology of Belgium consists of Palaeozoic rocks unconformably overlaid with almost flat lying layers of Mesozoic and Cenozoic soft rocks and sediments in a large part of the country (Fig.1). The basement of Palaeozoic age, generally folded, is made up of two main geological domains:

- the Lower Palaeozoic massifs (London-Brabant Massif, Stavelot Massif, Rocroi, Serpont and Givonne massifs) are composed of slates and quartzites which were deformed during the Caledonian orogeny (about 410 My ago). The most important massif is the London-Brabant Massif (Brabant Anticlinorium) in north Belgium, which is mostly overlaid by slightly tilted post-Palaeozoic layers. The thickness of these more or less compacted deposits (Cretaceous chalk, Tertiary sands and clays, Quaternary loess) increases towards the North with a maximum of more than 1000m in the Campine Basin. The Lower-Palaeozoic rocks of the Brabant Massif only outcrop in valleys where the Cenozoic cover has been eroded. Several faults with different orientations and variable dip cross the London-Brabant Massif (Legrand (1968) and Devos et al. (1993)).
- the Upper Palaeozoic (Devono-Carboniferous) formations, which constitute the northern part of the Rhenohercynian belt, were deformed during the Variscan orogeny. These calcareous and siliciclastic rocks rest unconformably on the Lower Palaeozoic massifs. A major fault, the Midi-Eifel-Aachen thrust-complex, which approximately coincides with the limit of the North Variscan Front, crosses Belgium from East to West (Fig. 1). North of this thrust, a foreland basin (The Namur Synclinorium) developed during the Variscan orogeny. Further North, Devono-Carboniferous rocks form the Campine basin which has not been deformed during the Variscan orogeny. To the South of the Midi Fault, the fold-and-thrust belt is composed of different structural units, which are, from North to South, the Dinant Synclinorium, the

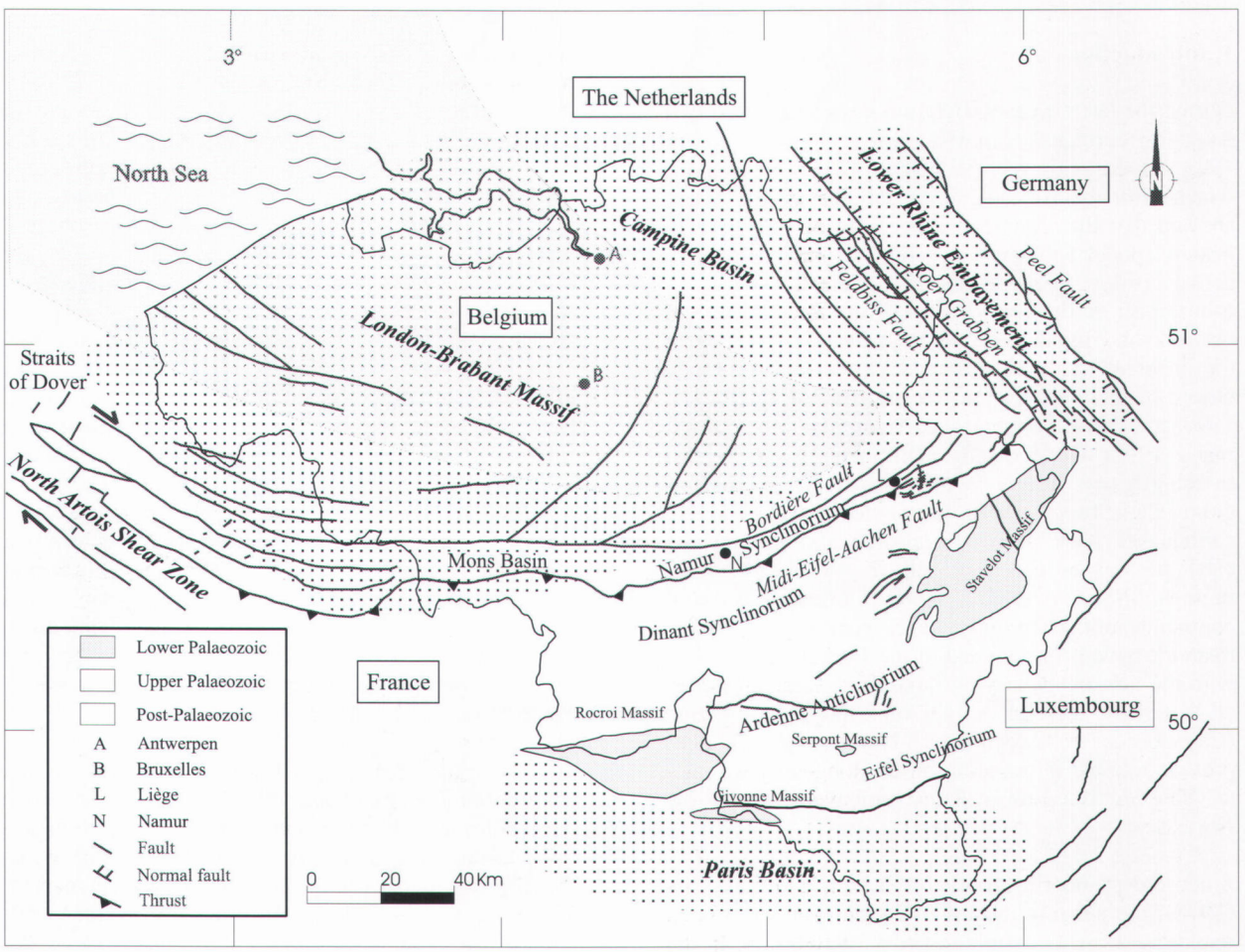

Figure 1. Schematic geological map of Belgium (redrawn from Legrand (1968), Colbeaux (1977 and 1980) and Geluk et al. (1994))

Ardenne Anticlinorium and the Neufchateau-Eifel Synclinorium. The southern part of this last unit is covered by post-Palaeozoic deposits of the Paris Basin. All these Palaeozoic formations are crossed by thrust and strike-slip faults which were activated during the Variscan orogeny (from 330 Ma to 290 Ma). No evidence of Pleistocene and Holocene activity is known along these faults.

More or less parallel to the Midi-Eifel-Aachen thrust-complex, the so-called Bordière Fault (Legrand, 1968) is supposed to follow the northern boundary of the Namur Synclinorium. This fault and the Midi-Eifel-Aachen thrust-complex are grossly in line with the North_Artois dextral shear zone defined in the North of France (Colbeaux, 1977). Paleo-stress field studies (Vandycke S. et al., 1988) have shown that the Mons basin structure could be considered as a pull-apart basin related to this major shear zone. In the Pas-de-Calais region, a NE-SW trending fault zone " la zone faillée du Pas-de Calais "(Colbeaux et al., 1980), may be associated with the block-faulting system in northern France and southern Great Britain and with a possible graben in the Channel.

To the NE of Belgium and in Southern Netherlands, several NW-SE trending quaternary normal faults delimit the Lower Rhine Graben (or Roer Valley Graben), filled with up to 2000 m of predominantly Upper Oligocene to Quaternary sediments (Geluk et al., 1994). The principal faults limiting the western and eastern boundaries of the graben are the Feldbiss Fault (Belgium) and the Peel Fault (The Netherlands), respectively. Slip on the Peel Fault was responsible for the 1992 Roermond earthquake (Ms=5.4). On the Belgian side, the Feldbiss Fault has been recognised as an active Quaternary fault (Camelbeeck and Meghraoui, 1996 and 1998). More to the South, outside the graben, several faults with similar orientation (NW-SE) were pointed out in the Stavelot-Venn Massif from geomorphological studies (Demoulin, 1988).

2.2. Geophysical data

Gravimetric and aeromagnetic data in Belgium have been processed and interpreted by De Vos et al. (1993) and more recently by Mansy et al. (1999) who presented new maps for Belgium and the surrounding areas. The main geophysical features interpreted by Mansy et al. (1999) are shown in Fig. 2. As the observed geophysical anomalies are generally related to pre-Cenozoic structures, only the main aspects are briefly outlined in this paper. The Bouguer anomaly map shows a strong difference between the northern and southern parts of Belgium. The northern area corresponds to a high gravity zone with, in its southwestern part, a WNW trending negative anomaly which is generally associated to a deep-seated granitic intrusion of late Ordovician to early Silurian age (Everaerts, 1996). On the contrary, the South of Belgium corresponds to a negative gravity anomaly. The high and low gravity zones are separated by a pronounced east-west gradient corresponding to the Bordière Fault (Chacksfield et al., 1993), juxtaposing the dense rocks of the London-Brabant Massif from the less dense Upper Palaeozoic rocks of southern Belgium.

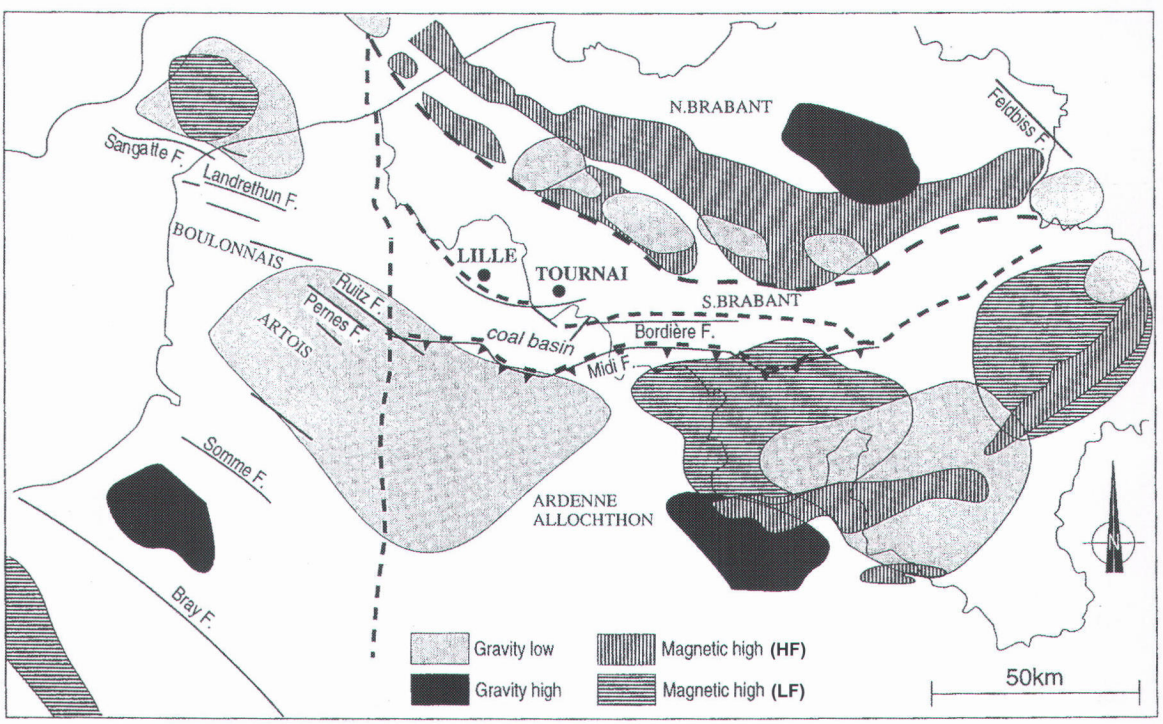

Figure 2. Main features from magnetic and gravity data (from Mansy et al, 1999). HF: High Frequency. LF: Low Frequency.

Magnitude threshold	1.8	3.3	4.7
Initial date for completeness	1985	1911	1350

Table 1. Magnitude thresholds and dates for the completeness of the earthquake catalogue in Belgium.

On the aeromagnetic map, the Lower Palaeozoic rocks of the London-Brabant Massif are outlined by positive magnetic anomalies oriented NW. To the east, the anomaly roughly trends EW. In the Ardennes domain, magnetic highs appear along the Lower Palaeozoic massifs, superposed on two large scale positive anomalies interpreted as a deep-seated Precambrian crustal block (Chacksfield et al., 1993).

3. Seismicity

The earthquake catalogue of the Royal Observatory of Belgium was used for this study. It includes the instrumental seismicity recorded since 1911 and the major historical earthquakes since 782. According to P. Alexandre (personal communication), all events with MSK intensity equal or higher than VII are listed since 1350. In order to ensure the completeness of the used data set, only the historical events meeting these criteria are considered in the following. In the catalogue, earthquakes are generally characterised by their local magnitude M_L which was converted to surface wave magnitude (M_S) using the relationship proposed by Ambraseys (1985) for Northwestern European earthquakes:

$$M_S = 0.09 + 0.93\ M_L \qquad (1)$$

The location and magnitude map of the earthquakes is presented in Fig. 3. The seismic activity is mainly located in the Roer Valley graben area, to the East of Belgium (Hautes-Fagnes area) and across the Mons Basin (Hainaut region). Several earthquakes with M_S magnitude ranging between 4.5 and 6.0 have been observed in and around Belgium since the seventeenth century. The main historical earthquakes in Northwestern Europe are listed in Camelbeeck and Meghraoui (1998). Among these, the following earthquakes have particularly affected Belgium : the three shocks having occurred in the southern part of the North Sea in 1382 (M_S ~ 6.0), 1449 (M_S ~ 5.5) and 1580 (M_S ~ 6.0), the Verviers (east of Belgium) 1692 earthquake (M_S 6.0 – 6.5), the 1756 Düren (Germany) earthquake (M_S ~ 5.5), the 1828 Tirlemont event (M_S ~ 4.6), the Oudenaerde earthquake (1938, M_S = 5.0), the Liège event (1983, M_S = 4.6) and the Roermond 1992 earthquake (M_S = 5.4). Smaller earthquakes in Hainaut were also damaging relatively small areas, like the Havré 1949 event, and the Carnières and La Louvière earthquakes in 1967 and 1968, respectively.

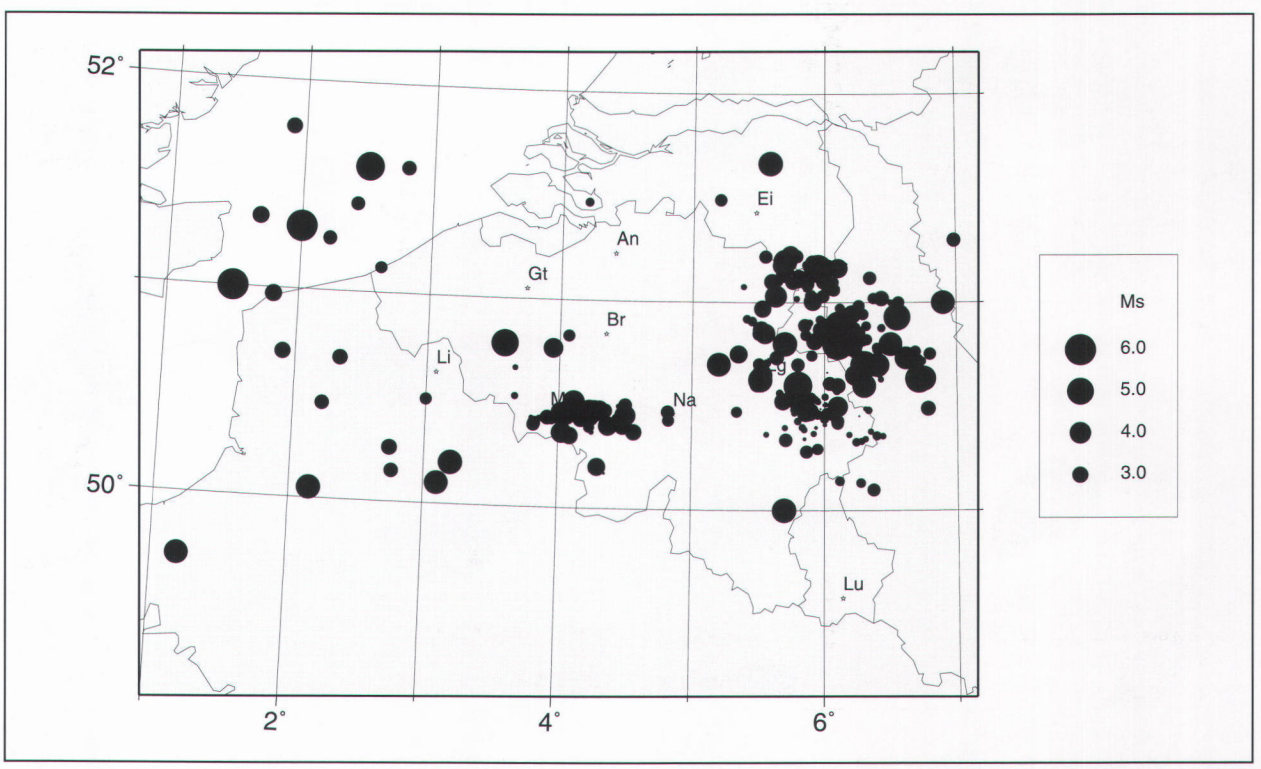

Figure 3. Seismic activity from instrumental seismicity (1911-1998) and large historical earthquakes (1350-1910)

4. Definition of seismic source zones

As Belgium is located in an intraplate area characterised by low tectonic deformation rates, the seismic activity is relatively low and diffuse, making difficult the definition and the location of seismic source zones. Except for the Roer Valley graben area, the seismic activity map does not show clear links between earthquake location and known faults for the considered time period (about 650 years). The seismic source zones have then been defined from the earthquake location and from the geological and geophysical data which give the limits of the crustal blocks. There is however a large uncertainty and subjectivity on the number and limits of the zones. Two different models have been defined. In the first approach, the minimum number of zones was considered, taking mainly into account the earthquake epicentre distribution (Model 1: Fig. 4). The source areas are the Roer Valley graben (1), the Liège zone (2), the Hautes-Fagnes area (3), the Hainaut zone (4) and the Pas-de-Calais zone (5). The remaining seismicity is distributed over a large area (SLZ) covering Belgium and a part of the Northern France. In a second approach (Model 2: Fig. 5), additional zones were introduced: the Western Brabant Massif zone (6), the Artois zone (7), the Ardennes zone (8) and the Limburg zone (9). The influence of the zoning model on the seismic hazard map will be studied later.

The main features of the zones are the following:

Zone 1 (Roer Valley Graben): This NW-SE zone extends from Germany to the Netherlands along the Belgian border and is characterised by the highest activity of Northwestern Europe (earthquake of magnitude M_S = 5.5 during historical period) with focal mechanisms showing NE-SW extension. This area includes the 1992 Roermond earthquake, M_S = 5.4, 17 km depth (Camelbeeck et al., 1994). The northern boundary is defined from gravimetry map (Camelbeeck, 1994) which shows the limit of the graben structure, while the southern boundary is fixed by the seismic activity.
Zone 2 (Liège): This ENE trending zone follows the orientation of the major Variscan structures (Legrand, 1968) in the vicinity of Liège and is limited to the North by the Bordière fault and to the South by the Midi-Eifel-Aachen thrust complex. This zone is characterised by strike-slip earthquakes with thrust component, one of which is the 1983 Liège event, M_S = 4.7, 4 to 6 km of depth (Camelbeeck & De Becker, 1985).
Zone 3 (Hautes-Fagnes): This relatively active area is delineated to the East and to the North by the Roer Valley graben and the Liège area, respectively. In this zone occurred the 1692 earthquake with $M_S \approx 6.0$-6.5 (Camelbeeck et al., 1999) and a swarm of events during 1990-1991 period located along a NW-SE trending fault across the Stavelot massif (Demoulin, 1988). Focal mechanisms generally show strike-slip faults with a normal component or normal faults (Camelbeeck, 1994).
Zone 4 (Hainaut): This source area is defined by the relatively high seismic activity of this century located between Mons and Charleroi, to the South of the Bordière fault. The maximum M_S magnitude recorded in the area during this period is 4.3. On the contrary, no major historical earthquake (event giving an intensity equal or higher than VII) has been observed since 1350 (Camelbeeck & Meghraoui, 1998). The earthquakes recorded in this area are generally shallow (a few km deep).
Zone 5 (Pas-de-Calais): This zone includes the three historical shocks (M_S=5.5 to 6.0) that occurred in 1382, 1449 and 1580 (Camelbeeck & Meghraoui, 1998), and seems to be fall into a NE-SW line which could correspond to a graben zone located between England and the continent (Colbeaux, 1977). This relation is still unproven and there is no significant recent seismicity in this area. The mean source depth of the historical earthquakes has been estimated to 20 km from the isoseismal maps (Melville et al., 1996).
Zone 6 (Western Brabant Massif): It extends from the North of Liège to the North Sea and is defined by the NW-SE trending geophysical anomalies which also correspond to Palaeozoic faults in the Brabant Massif (Everaerts et al., 1996; Mansy et al., 1999). This zone includes the Oudenaarde earthquake (1938, M_S=5.0, 24 km depth) and the Tirlemont event (1828; M_S estimated to 4.6), as well as some minor shocks after 1910.
Zone 7 (Artois): This area shows a very diffuse seismicity limited to the North by the Nord-Artois strike-slip zone (Colbeaux, 1977). Two events with M_S estimated to 4.7 (Intensity VII) occurred in 1896 and 1783. The mean depth has been fixed to 10 km.
Zone 8 (Ardennes): This large zone shows a low seismic activity with a main historical event in 1733 (Bastogne earthquake, with a maximum intensity of VII and M_S estimated to 4.7). It extends from the eastern boundary of the Artois zone to the west of the Hautes-Fagnes source zone.
Zone 9 (Limburg): This area is delineated to the NE by the Roer Valley Graben and to the South by the Liège zone. The western limit is defined by the seismicity and the Rauw fault (Geluk et al., 1994), which is parallel to the fault system of the graben.

In both models, a background seismic zone with a maximum earthquake magnitude of 3.0 was defined to account for the floating earthquakes not considered by these sources.

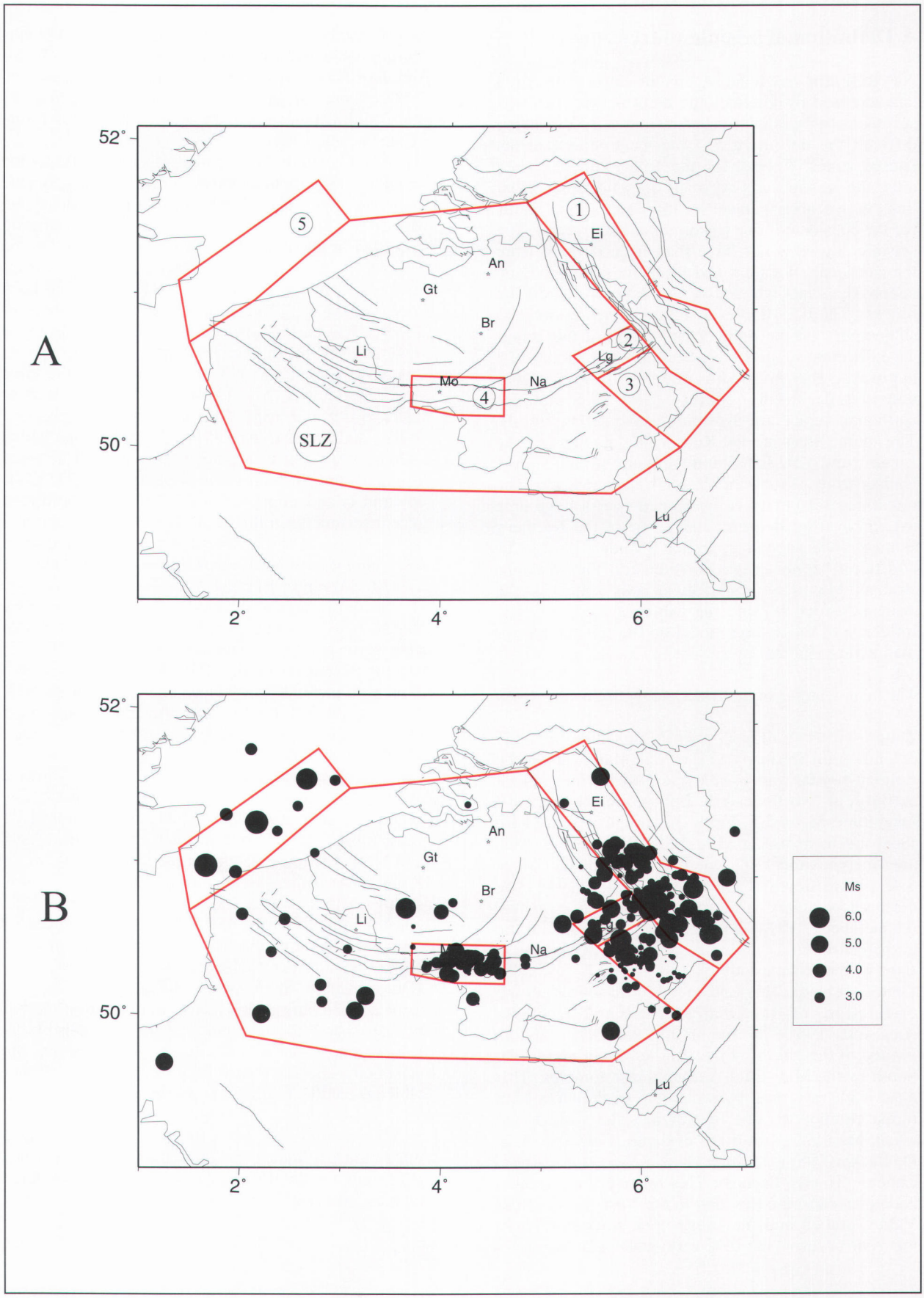

Figure 4. Model 1: (A) six seismic source areas in and around Belgium. (B) the same with seismicity.

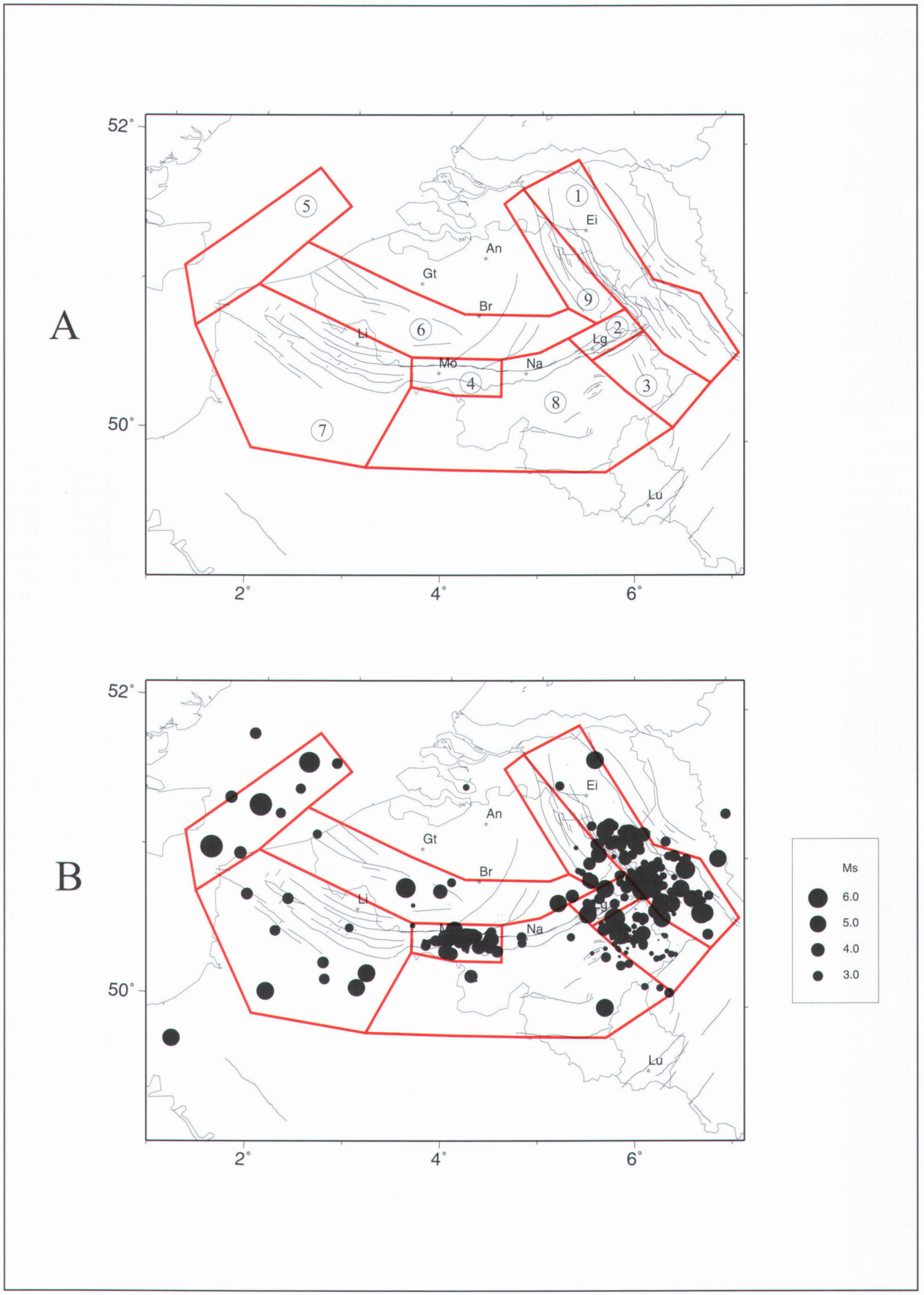

Figure 5. Model 2: (A) nine seismic source areas in and around Belgium. (B) the same with seismicity.

5. Seismic zone characterisation

5.1. Seismic activity

The seismic activity of a region can be represented by the cumulative annual rate of earthquakes with magnitude greater or equal to a specific M_S value, the so-called Gutenberg-Richter relation ship:

$$\log N = a - bM_S \qquad (1)$$

where N is the cumulative number of events per year with magnitude equal to or larger than M_S, a and b are two constants determined from the data set. The a value represents the average number of earthquakes of magnitude 0 and greater while the b value, which is the slope of the line, indicates the relative number of large and small earthquakes.

The earthquake catalogue is not homogeneous and the data quality strongly varies with time, improving with the apparition of instruments and the development of the Belgian seismological network. As mentioned before, all earthquakes giving an intensity equal to or greater than VII are supposed to be known since 1350 (Alexandre, personal communication). From the catalogue, an intensity of VII is generated by an earthquake with a magnitude of about 4.7, similar to the Liège event (1983). From 1911, the magnitude threshold decreases to 3.3 (Camelbeeck, 1994) with the installation of the first seismographs. A second major improvement occurred in 1985 with the development of the Belgian network after the Liège earthquake, which allows to detect all the events with a magnitude equal to or greater than 1.8.

Assuming the completeness of the catalogue for the three periods and the corresponding magnitudes, the seismic activity has first been estimated for the whole data set, excluding fore and aftershocks. The Gutenberg-Richter law, using the least-squares method, is the following (Fig. 6a):

$$\log_{10} N = 2.7 - 0.87M_S \qquad (2)$$

with a correlation coefficient of 0.997. The fitting of equation (2) to the data is very good and it gives a first evaluation of the seismic activity for Belgium.

In seismic hazard assessment, the activity inside each seismic zone has to be evaluated before the computations. As the earthquake number in some zones is small, it is hazardous to define a specific b value. The frequency-magnitude law is then determined keeping the b-parameter (-0.87) constant and estimating a new a-parameter to fit the observed data in each zone (Figs. 6b to 6k). The Gutenberg-Richter parameters for each zone are given in Table 2, as well as the maximum magnitude and the source depth. For the seismic zones with a high activity (Roer Valley graben, Hautes-Fagnes), a reliable estimation of the a parameter can be obtained (Figs. 6b and 6e). In all the other zones, the uncertainty on a is higher, due to the lack of data or the competition between data at different periods. The first example is the Hainaut area (Fig.6d) where no event with an intensity equal to or greater than VII (assumed magnitude of 4.7) has been observed for 648 years. The occurrence of one such earthquake is represented by a black square in the Gutenberg-Richter diagram. A clear opposition appears between the earthquake occurrences in the different magnitude ranges when considering a b-value

Zone	Zone Name	Observed M_S		M_S max evaluated	$\log_{10} N = a - bM_S$		Source Depth
		historical	instrumental		a	b	
1	Roer Valley graben	5.5 (1756)	5.4	6.6	2.4	-0.87	15 km
2	Liège	(?)	4.7	5.2	1.5		5 km
3	Hautes-Fagnes	6.0-6.5 (1692)	4.1	6.5	1.7		10 km
4	Hainaut	(?)	4.3	4.5	2.0		5 km
5	Pas-de-Calais	6.0 (1382, 1580)	3.3	6.5	2.3		20 km
6	west Brabant massif	4.6 (1828)	5.0	5.5	1.7		20 km
7	Artois	4.7 (1783, 1896)	3.3	5.2	1.4		10 km
8	Ardennes	4.7 (1733)	< 3.0	5.2	1.4		10 km
9	Limburg	(?)	4.3	4.8	1.5		10 km
SLZ	Single Large Zone (Model 1)	4.7	5.0	5.5	2		10 km

Table 2. Characteristics of the seismic zones.

of –0.87 . Earthquakes with magnitude values between 2.9 and 4.2 are more numerous than the stronger and weaker ones, considering the Gutenberg-Richter law. The relatively numerous intermediate earthquakes of this century occurred during an intensive coal mining exploitation but no clear link has been shown so far between seismic activity and mining. The chosen line defines a moderate activity (a=2.0) compared to the activity (a=2.2) derived from the intermediate earthquakes. On the other hand, a lower b-value could be considered to better fit the seismic data in the Hainaut area. At this stage, we decided to keep the same b-value but the activity of this area should be studied with more details. In the Liège area, all the earthquakes, less numerous than in the Hainaut zone, have also been observed after 1911 and the scarcity of the data does not allow an easy fitting of a line (Fig. 6f). As only one earthquake of magnitude greater than or equal to 4.7 (the Liège earthquake of 1983) has affected the area since 1350, the line defining the seismic activity must be below the square which corresponds to the occurrence of two events of Ms≥4.7 between 1350 and 1998. Some areas are characterised by very few data and the choice of the a parameter is very subjective, particularly in the Brabant and Artois zones (Figs. 6g and 6i).

5.2. Upper bound magnitude and source depth

The maximum possible earthquake within each seismic zone has to be chosen. It is a parameter difficult to estimate, particularly in low strain-rate intraplate areas where data are lacking. Three methods have been proposed (Bollinger et al., 1992) for determining the maximum magnitude earthquake in such areas: (1) addition of an increment (0.5 to 1 magnitude units in practice) to the largest historical earthquake, (2) extrapolation of the magnitude recurrence relations and (3) the use of known or estimated source dimensions.

In this study, the first method was used in most zones by adding 0.5 magnitude unit to the largest earthquake. In the Roer Valley graben, the maximum magnitude was determined from the results of the paleoseismological study carried out along the Feldbiss fault (Camelbeeck & Meghraoui, 1998), which estimates the maximum magnitude close to Ms=6.6. Finally, in the Hainaut zone, the upper bound magnitude has been fixed to 4.5 (instead of 4.8), considering the low seismic activity for magnitudes higher than 4.0 in this area during 648 years.

The depth of the earthquakes is another key parameter intervening in the seismic hazard analysis through the attenuation law. In Belgium, significant contrasts appear between the source depths within the same region and a mean source depth has been estimated for each seismic zone from the events correctly located in the catalogue. The source depth values for each zone are listed in the table 2.

6. Applicable attenuation relationships

The earthquake hazard analysis requires an estimate of ground motion as a function of distance from a specified earthquake. The attenuation relation ships which provide the vertical or horizontal peak ground acceleration as a function of magnitude, source depth, distance and site conditions are generally semi-empirical equations derived from a strong motion data set. No strong motions are available in Belgium and we have used the predictive relationships proposed by Ambraseys (1995) and Ambraseys et al. (1996) for shallow earthquakes in the European area. The first attenuation law (1995) is based on a data set of 1260 strong motion records generated by 619 shallow earthquakes in the European area.

For horizontal acceleration on the rock, the attenuation relationship is given by the following equation which accounts for the focal depth:

$$\log_{10}(a_h) = -1.06 + 0.245M_S - 1.016\log_{10}(r) - 0.00045r + 0.25P \quad (3)$$

where a_h is the peak horizontal acceleration in g, M_S is the surface wave magnitude, $r = \sqrt{d^2 + h^2}$, d is the shortest distance from the station to the surface projection of the fault rupture and h is the focal depth. The standard deviation of $\log(a_h)$ is 0.25, and P=0 for 50-percentiles and P=1 for 84-percentiles.

In 1996, Ambraseys et al. provided a second predictive peak ground acceleration attenuation relationship, from 422 triaxial records generated by 157 earthquakes in Europe and adjacent regions with surface wave magnitude between 4.0 and 7.9. In that study, the local soil conditions are considered and the focal depth does not appear explicitly in the equation which is:

$$\log(a_h) = -1.48 + 0.266M_S - 0.922\log(r) + 0.117S_A + 0.124S_S + 0.25P \quad (4)$$

where a_h is the peak horizontal acceleration in g, M_S is the surface wave magnitude, $r = \sqrt{d^2 + h_o^2}$, d is the shortest distance from the station to the surface projection of the fault rupture, h_o is a constant equal to 3.5, P=0 for mean values , P=1 for 84-percentile values of $\log a_h$, S_A = 1 for stiff soil sites (Vs=360-750 m/sec) and S_A = 0 otherwise, Ss = 1 for soft soil sites (Vs=180-360 m/sec) and Ss = 0 otherwise, Vs is the shear wave velocity.

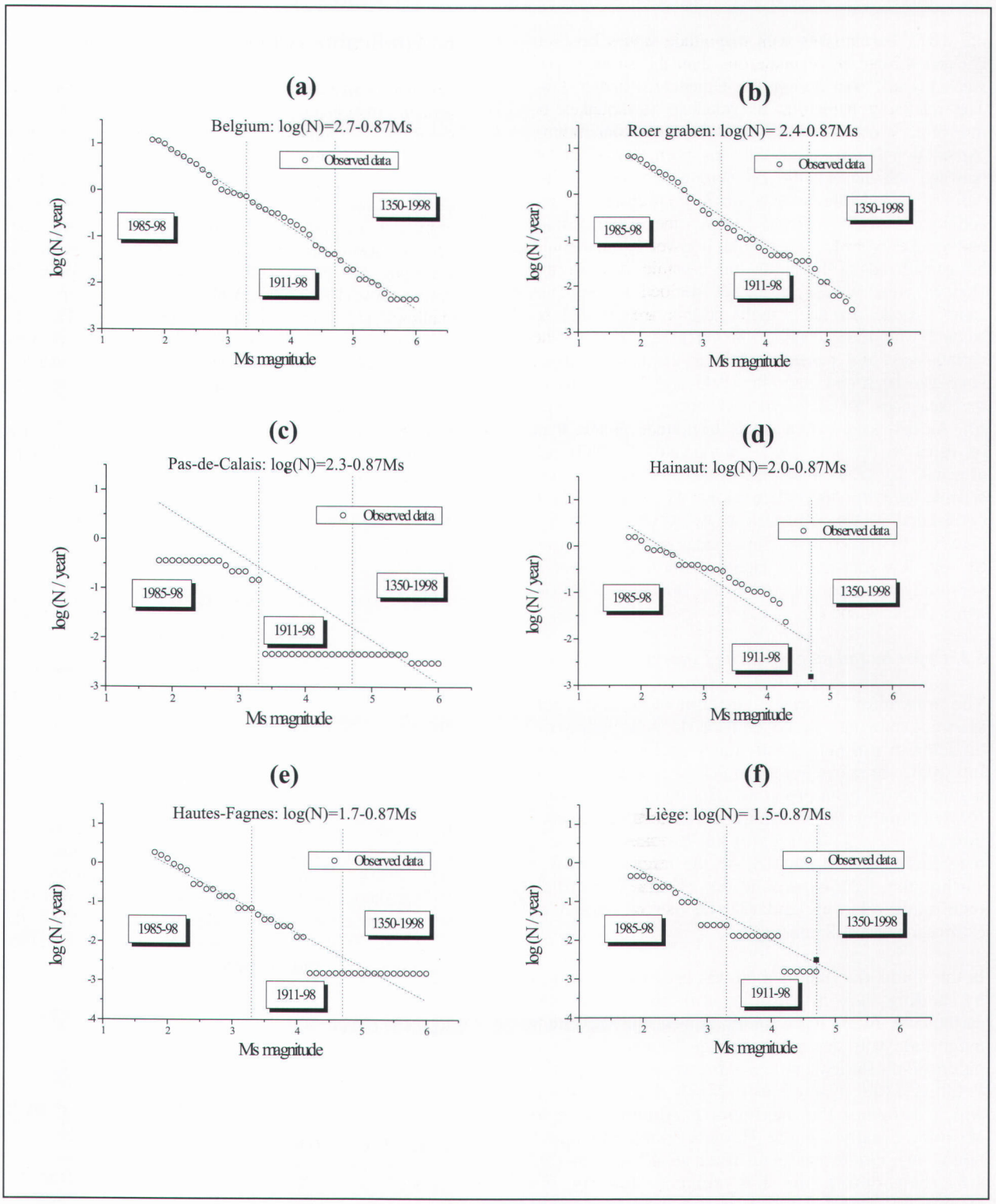

Figure 6. Gutenberg-Richter relationships for all the catalogue data (a) and for the different seismic source zones (b to k). The dashed line represents the chosen recurrence law. The magnitude range has been split in three parts corresponding to period times for which completeness is assumed.

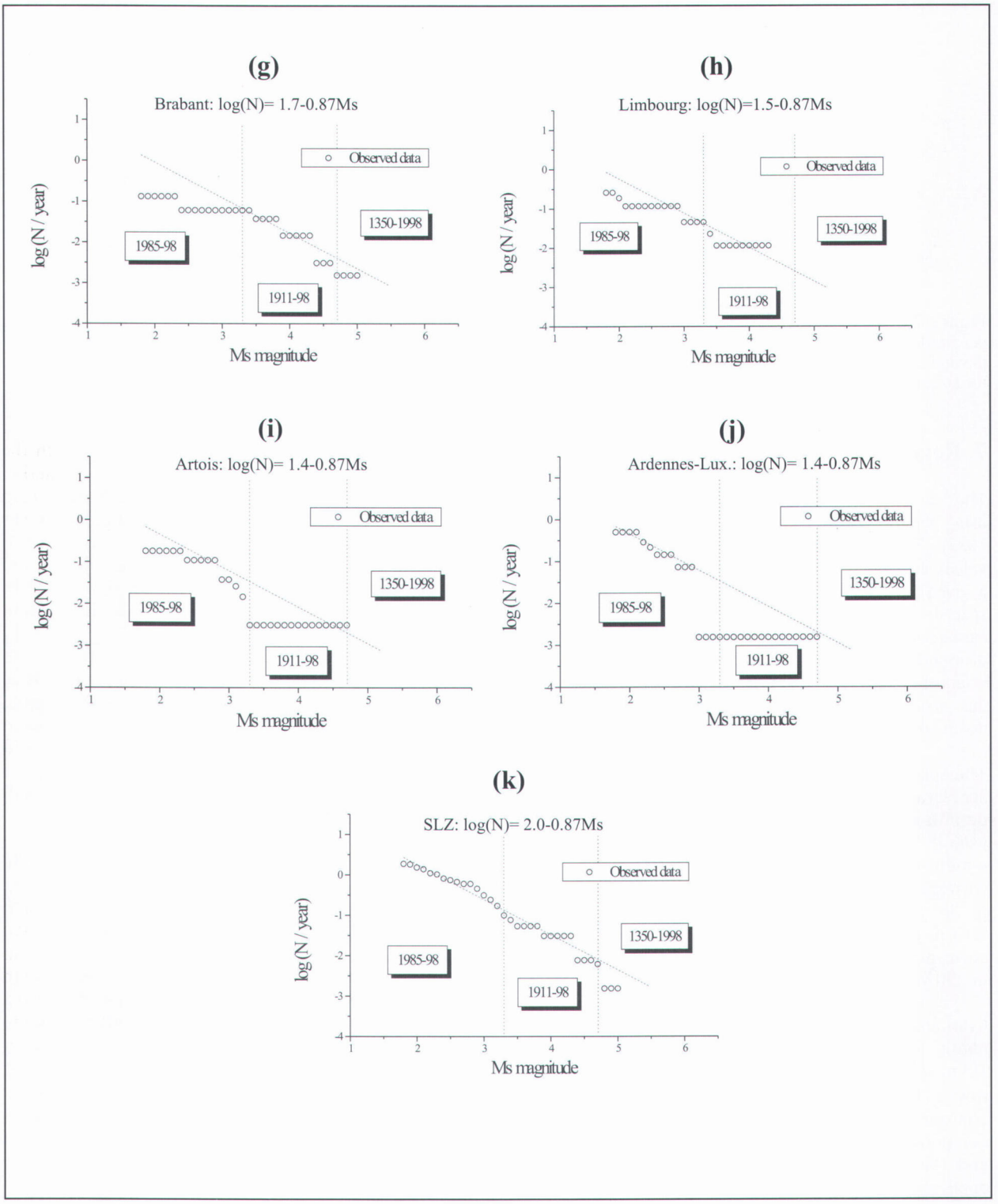

The attenuation curves predicted by equation (3) on rock sites for the 50-percentile values are presented in Fig. 7 for different focal depth values (5, 10, 15 and 20 km) and are compared with equation (4). The dramatic effect of focal depth on the ground acceleration at short epicentral distance is clearly evinced. The shallower the earthquake, the higher is the horizontal peak ground acceleration. Of course, this comparison does not hold for strong earthquakes initiated at depth and causing ruptures at the surface. In this case, equation (4) should be considered. The scattering of the data is illustrated in Fig. 8 which shows the two attenuation laws defined by eqs. (3) and (4) with and without standard deviation. Considering one standard deviation almost doubles the ground acceleration values at any distance.

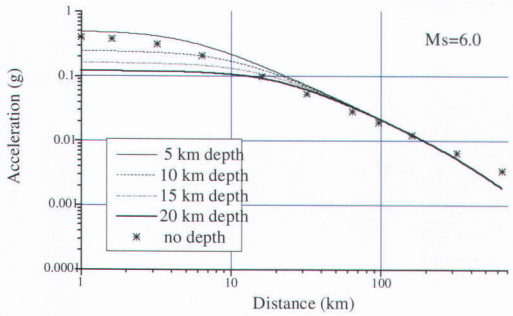

Figure 7. Ambraseys's attenuation laws for the 50-percentile acceleration values, considering the influence of the depth (5 km to 20 km in equation 3) or not (equation 4), for an earthquake of magnitude Ms=6.0.

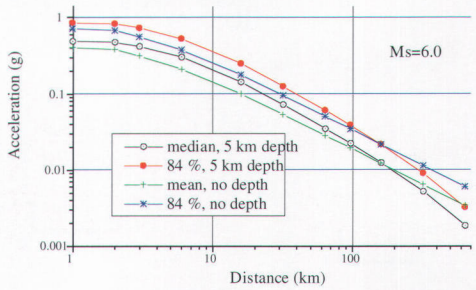

Figure 8. Ambraseys's attenuation laws (with depth and without depth control) taking into account or not a standard deviation in equations 3 and 4, for an earthquake of magnitude Ms=6.0.

7. Regional seismic hazard assessment

The seismic hazard assessment has been computed using the SEISRISK III program (Bender & Perkins, 1987). This seismic code computes peak acceleration values that have a probability of non-exceedance during a given time period at each of a set of sites uniformly spaced on a two-dimensional grid. In this model, earthquake occurrences are assumed to have a Poisson distribution and the seismicity is assumed to be stationary during the time intervals being considered. In this regional scale study, the ground conditions are assumed to be rock, as requested by Eurocode 8.

The seismic hazard is represented by a peak ground acceleration map for a given return period (see definition in Appendix 1). In this study, maps have usually been computed for a 475 years return period which is the reference used in Eurocode 8. It corresponds to a non-exceedance probability of 90% in 50 years. For long-live constructions, another return period of interest is 2375 years, which corresponds to a non-exceedance probability of 90% in 250 years.

Computations were performed for the two models using parameters presented in table 2 over a 10km×10km grid with 44 N-S columns and 35 E-W rows. The acceleration values are given in g with a contouring interval of $0.02g$. Different maps were computed, varying the zone model, the return period and the attenuation laws (with or without source depth and standard variation).

The first two seismic hazard maps (Figs. 9A and 9B) were calculated for a return period of 475 years, considering a median attenuation law without source depth effect (equation 4). The only difference between the two maps is the input zone model. For Model 1 (Fig. 9A), the largest acceleration values (over 0.06 g) are reached in the eastern part of Belgium (Roer Valley graben area, Liège and Hautes-Fagnes areas), in the Hainaut basin and in the Pas-de-Calais area. These higher acceleration values correspond to the zones with a high a-value in the Gutenberg-Richter law (Table 2). When considering the other zones (Model 2, Fig. 9B), the hazard map is very similar. In a second step, the source depth was taken into account in the attenuation law (equation 3) and the results for the same input parameters are compared for the two models in Figs. 10A and 10B. In this case, the highest peaks occur in the Hainaut and Liège areas with acceleration values over 0.1g and 0.08g, respectively. These spots correspond to the zones with a relatively high and shallow seismic activity, highlighting the effect of the source depth. Again, the difference between the two maps obtained for the two models is not significant, as was also shown by other tests not presented here. In the following, only one of these models (Model 2) will be considered in the computations.

If one standard deviation is introduced in the attenuation law (84-percentile values, Fig. 11B), a strong and not homogeneous increase of acceleration values is observed (compare Figs. 10B and 11B), with acceleration maxima over 0.14g and 0.12 g in the Hainaut and Liège areas. Without source depth control in the attenuation law (equation 4, Fig. 11A), the three zones already evinced in Fig. 9B present the highest seismic hazard with acceleration values over 0.1g. The differences between Figs. 11A and 11B clearly illustrate the influence of the source depth which increases the seismic hazard in the Hainaut and Liège areas. On the contrary, this latter is relatively lower in the Roer Valley graben a priori characterised by deeper sources.

Finally, two hazard maps (Model 2, 84% attenuation law) considering or not the effect of source depth were computed for a return period of 2375 years which corresponds to 90% probability of non-exceedance during 250 years. The results (to be compared to Figs. 11A and 11B for a return period of 475 years) globally show a relatively homogeneous increase of the acceleration values which reach 0.2 g in the Roer Valley graben area (Fig. 12A, no depth), 0.26 and 0.22 g in the Hainaut and Liège areas respectively (Fig. 12B, depth control).

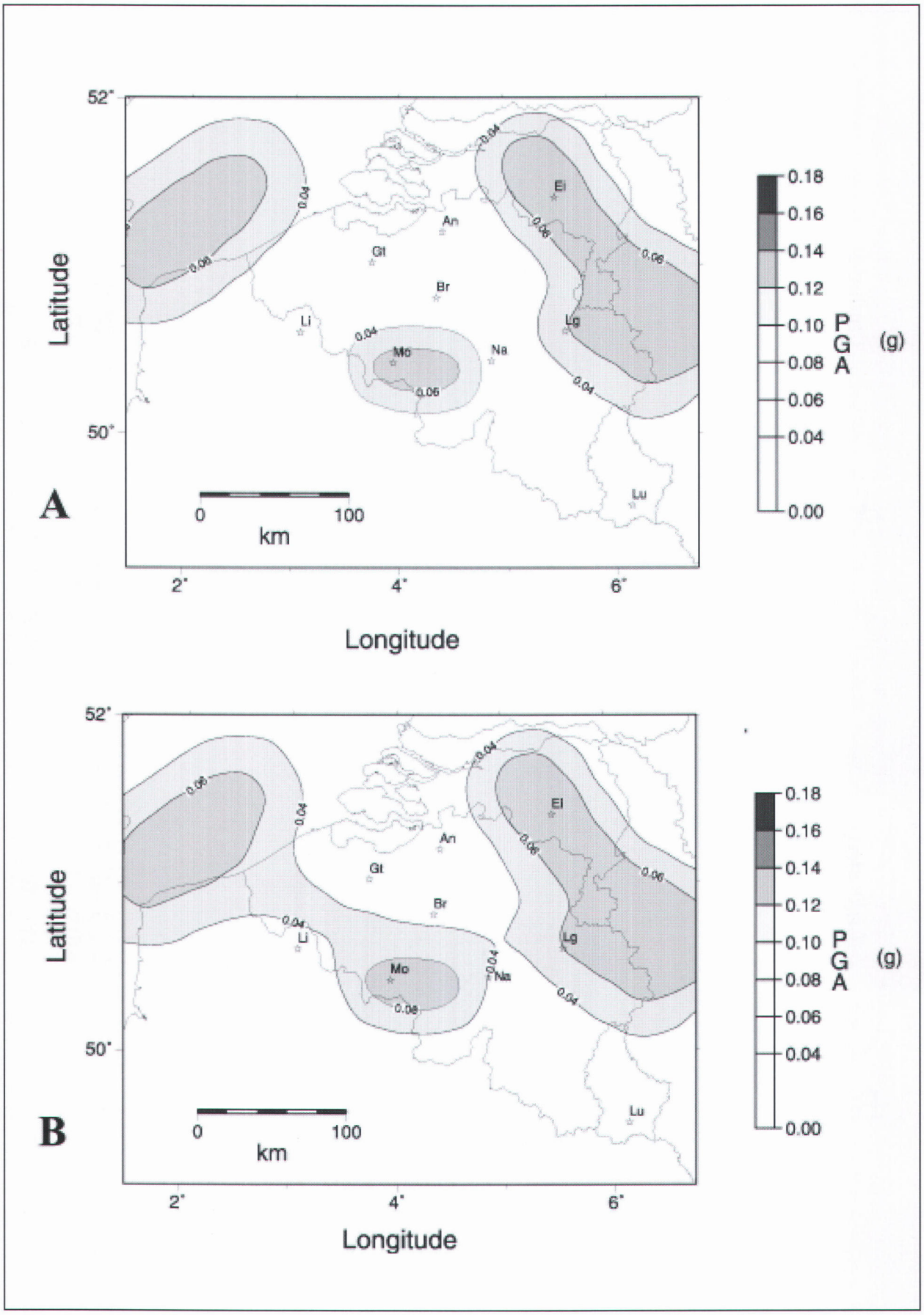

Figure 9. Peak Ground Acceleration (PGA) on rock with 90% probability of non-exceedance during 50 years (475-year return period). (A) Model 1. (B) Model 2. The effect of the depth source is not considered in the attenuation law (eq. 4).

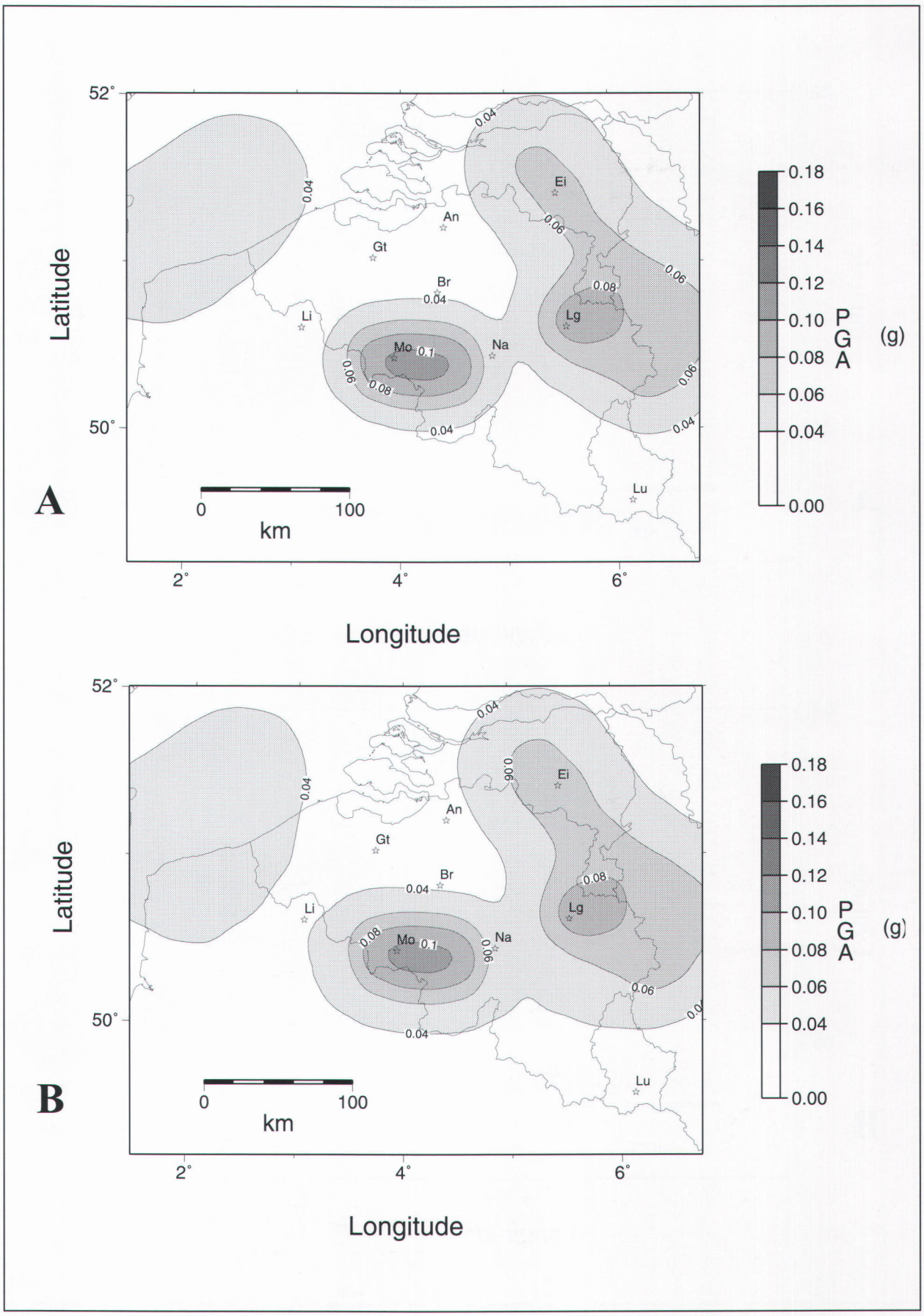

Figure 10. Peak Ground Acceleration (PGA) on rock with 90% probability of non-exceedance during 50 years (475-year return period). (A) Model 1. (B) Model 2. The effect of the depth source is considered in the attenuation law (eq. 3).

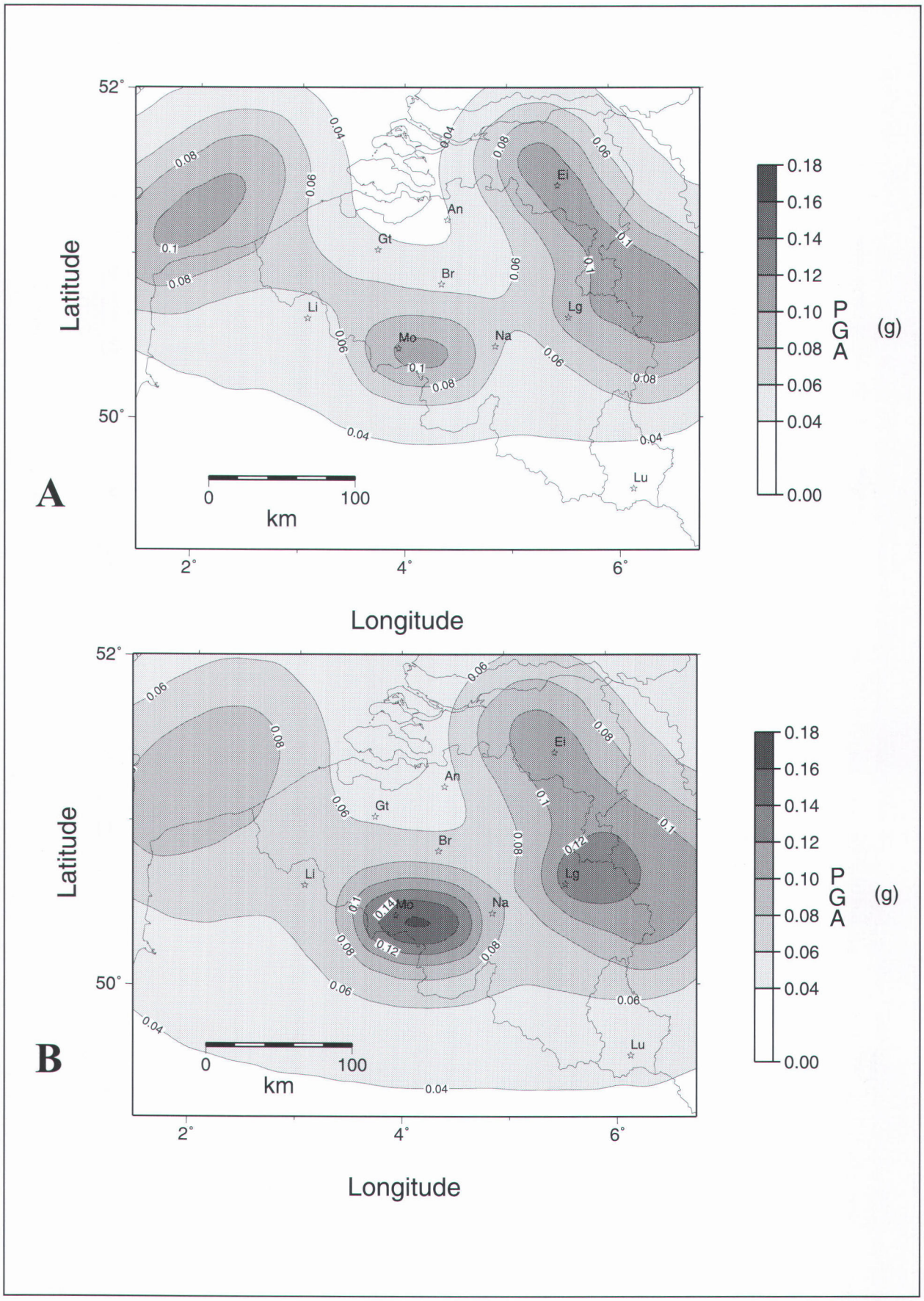

Figure 11. Peak Ground Acceleration (PGA) on rock with 90% probability of non-exceedance during 50 years (475-year return period). Model 2, Ambraseys attenuation law with standard deviation (84%). (A): without depth control, (B) with depth control.

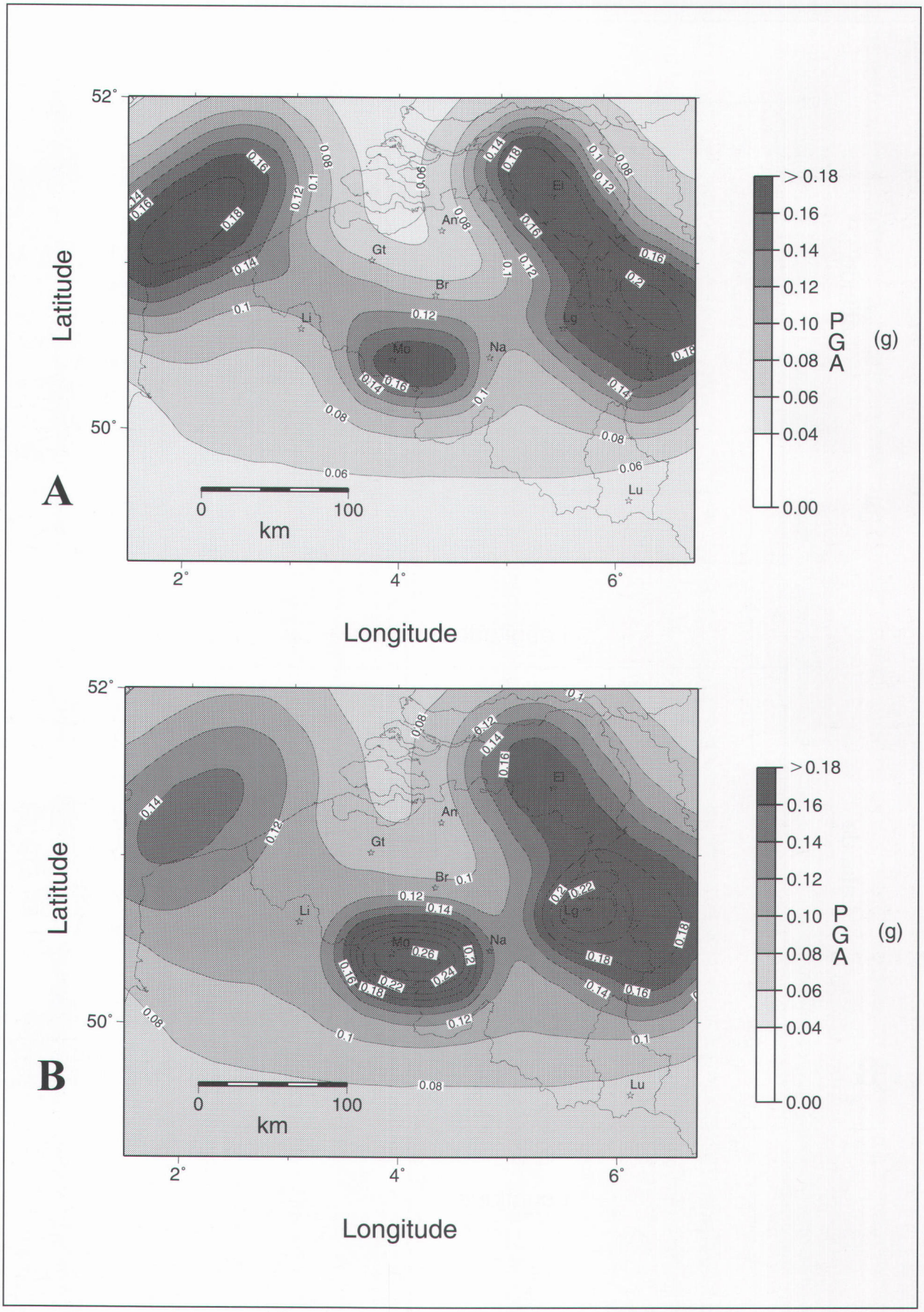

Figure 12. Peak Ground Acceleration (PGA) on rock with 90% probability of non-exceedance during 250 years (2375-year return period). Model 2, Ambraseys attenuation law (84%). (A) without depth control, (B) with depth control.

8. Results and conclusions

The regional seismic hazard has been assessed for Belgium and seismic hazard maps have been elaborated for a return period of 475 years and rock conditions, as required by Eurocode 8. Hence, the computed peak acceleration values do not take into account the site effects resulting from the presence of soft sedimentary layers overlaying the rock. This effect is certainly strong in Belgium where a large part of the country is covered by Mesozoic and Cenozoic soft deposits. In Eurocode 8, this effect is considered in the response spectra proposed for different soil conditions.

A large number of uncertainties appeared at the different stages of this work, in the definition of the seismic source areas, the source characterisation and the definition of attenuation law. The line followed at the different steps of the work aimed at making clear and reasonable choices in order to propose a non-exaggerated level of seismic hazard. It is clear in our mind that the proposed maps just constitute a first step to evaluate the seismic hazard in Belgium and that they will evolve with new geological and seismological data.

Two zone models were considered at the beginning of the study, owing to the difficulty of defining seismic zones in an intra-plate area like Belgium. The results obtained with both models are very similar and it has turned out that there is no need to refine the definition of seismic sources with the present day seismological and geological data.

A Gutenberg-Richter law has been determined for whole Belgium using seismological data. Making distinction of seismological observations on different periods, the magnitude-frequency relation estimated fit very well the data with $b = -0.87$. For each zone, the seismic activity is more difficult to evaluate, particularly for the Hainaut source zone.

Finally, the attenuation laws have appeared to have a large influence on the computed acceleration values, which are particularly dependent of the source depth. Without depth control, the seismic hazard is the highest in three main areas (Roer Valley graben and Liège area, Hainaut and Pas de Calais), corresponding to the source zones with the strongest activity. If the source depth is considered in the computations, high acceleration spots appear in the zones with shallow seismic sources (Hainaut and Liège areas, epicentres at 5 km depth). Most of the damaging earthquakes that occurred during historical times were located in the eastern part of Belgium (from Liège to the German border) and in the Hainaut region, and the seismic hazard map for a return period of 475 years (Fig. 11B) is coherent with this short-term image of the seismic activity. This map was computed using an attenuation law with one standard deviation (84 percentiles) to account for the large uncertainty on the strong motion data.

9. Acknowledgments

This study was funded by a contract with the Scientific and Technical Centre for Construction (Brussels) and the Belgian Ministry of Economical Affairs. We also want to thank all the members of the Belgian NAD committee for the fruitful discussions about the seismic hazard in Belgium.

10. References

ALEXANDRE, P., 1994. Historical seismicity of the lower Rhine and Meuse valleys from 600 to 1525: a new critical review, *Geologie en Mijnbouw*, 73: 431-438.

AMBRASEYS, N.N., 1983. Evaluation of Seismic Risk, in the proceedings of the NATO advanced research workshop on Seismicity and seismic risk in the Offshore North Sea area, Ritsema and Gurpinar eds., June 1-4 1982, NATO series 99, 317-345.

AMBRASEYS, N.N., 1985. Magnitude assessment of Northwestern European Earthquakes. *Earthquake Engineering and Structural Dynamics*, 13: 307-320.

AMBRASEYS, N.N., 1995. The prediction of Earthquake Peak Ground Acceleration in Europe. *Earthquake Engineering and Structural Dynamics*, 24: 467-490.

AMBRASEYS, N.N., SIMPSON, K.A. & BOMMER, J.J., 1996. Prediction of horizontal response spectra in Europe. Earthquake Engineering and Structural Dynamics, 25: 371-400.

BENDER, B. & PERKINS, D.M., 1987. SEISRISK III: A computer Program for Seismic Hazard Estimation. *U.S. Geological Survey Bulletin*, 1772.

BOLLINGER, G.A., SIBOL, M.S. & CHAPMAN, M.C., 1992. Maximum magnitude estimation for an intraplate setting: example: the Giles County, Virginia, seismic zone. *Seismological Research Letters*, 63: 139-152.

CAMELBEECK, T., 1990. L'activité séismique actuelle (1985-1988) en Belgique. Comparaison avec les données de séismicité historique et instrumentale. Analyse séismotectonique. *Annales de la Société Géologique de Belgique*, 112: 347-365.

CAMELBEECK, T., 1994, Doctorat en Sciences Physiques à l'UCL, « Mécanisme au foyer des tremblements de terre et contraintes tectoniques : le cas de la zone intraplaque belge », Observatoire Royal de Belgique, série Géophysique.

CAMELBEECK, T. & DE BECKER, M., 1985. The earthquakes of Liège of November 8, 1983 and December 21, 1965. In « Seismic activity in western Europe », editor P.Melchior, Reidel (1985): 233-248.

CAMELBEECK, T., VAN ECK, T., PELZING, R., AHORNER, L., LOOHUIS, J., HAAK, H.W., HOANG-TRONG, P. & HOLLNACK, D.,1994. The 1992 Roermond earthquake, the Netherlands, and its aftershocks. *Geologie en Mijnbouw,* 73: 181-197.

CAMELBEECK, T. & MEGHRAOUI, M., 1996. Large earthquakes in northern Europe more likely than once thought. *EOS, Transactions*, American Geophysical Union, 77: 405 and 409.

CAMELBEECK, T. & MEGHRAOUI, M., 1998. Geological and geophysical evidence for large palaeoearthquakes with surface faulting in the Roer Graben (northwestern Europe). *Geophysical Journal International*, 132 : 347-362.

CAMELBEECK, T., VANNESTE, K. & ALEXANDRE, P., 1999. L'Europe Occidentale n'est pas à l'abri d'un grand tremblement de terre. Ciel et Terre, 115: 13-23.

CHACKSFIELD, B.C., DE VOS, W., D'HOOGE, L., DUSAR, M., LEE, M.K., POITEVIN, C., ROYLES, C.P. & VERNIERS, J., 1993. A new look at Belgian aeromagnetic and gravity data through image-based display and integrated modelling techniques. *Geological magazine*, 130 (5): 583-591.

COLBEAUX, J.P., 1977. Géométrie et cinématique de la fracturation dans le Nord de la France. *Bulletin B.R.G.M.*, (2) section IV, 4 : 339-355.

COLBEAUX, J.P., DUPUIS, C., ROBASZYNSKI, F., AUFFRET, J.P., HAESAERTS, P. & SOMME, J., 1980. Le détroit du Pas-de-Calais: un élément dans la tectonique de blocs de l' Europe Nord-Occidentale. *Bulletin d'information des Géologues du Bassin de Paris*, 17 (4): 41-45.

COMMISSION OF THE EUROPEAN COMMUNITIES, 1993. Eurocode 8: Earthquake resistant design of structures. Part 1-1: Seismic actions and general requirements for structures.

CORNEL, C. A., 1968. Engineering seismic risk analysis. *Bulletin of the Seismological Society of America*, 58 (5): 1583-1606.

DEMOULIN, A., 1988. Cenozoic tectonics on the Hautes-Fagnes plateau (Belgium). *Tectonophysics*, 145: 31-41.

DE VOS, W., CHACKSFIELD, B.C., D'HOOGE, L., DUSAR, M., LEE, M.K., POITEVIN, C., ROYLES, C.P., VANDENBORGH, J., VAN EYCK J. & VERNIERS, J., 1993. Image-based display of Belgian digital aeromagnetic and gravity data. *Service Géologique de Belgique. Professional Paper*, 263.

EVERAERTS, M., POITEVIN, C., DE VOS, W., STERPIN, M., 1996. Integrated geophysical/geological modelling of the Western Brabant Massif and structural implications. *Annales de la Société géologique de Belgique*, 105: 41-59.

GELUK, M.C., DUIN, E.J.TH., DUSAR, M., RIJKERS R.H.B, VAN DEN BERG, M.W. & VAN ROOIJEN, P., (1994). Stratigraphy and tectonics of the Roer Valley Graben. *Geologie en Mijnbouw*, 73: 129-141.

JONGMANS, D. & CAMELBEECK, TH., 1989. Influence des structures géologiques à petite et grande échelle sur les mouvements de sol lors de tremblements de terre en Belgique. Colloque national du C.B.G.I., Sart Tilman-Liège, 17-18-19 octobre 1989, IV.13-IV.24.

JONGMANS, D. & CAMPILLO, M., 1990. The Liège earthquake of November 8, 1983, Damage distribution and site effects. *Earthquake Spectra*, 6 (4): 713-737.

JONGMANS D., 1991. L'influence des structures géologiques sur l'amplification des ondes sismiques. Mesures in situ et modélisations. Collection des publications de la Faculté des Sciences Appliquées n° 131, Université de Liège, 250 p.

LEE, M.K., PHARAOH, T.C., WILLIAMSON, J.P., GREEN, C.A. & DE VOS, W., 1993. Evidence on the deep structure of the Anglo-Brabant Massif from gravity and magnetic data. *Geological Magazine*, 130 (5): 575-582.

LEGRAND, R., 1968. Le Massif du Brabant. Mémoires pour servir à l'explication des Cartes géologiques et minières de la Belgique, 9, 148p.

MANSY, J.L., EVERAERTS, M., & DE VOS, W., 1999. Structural analysis of the adjacent Acadian and Variscan fold belts in Belgium and northern France from geophysical and geological evidence. *Tectonophysics*, 309 (1-4): 99-116.

MELVILLE, C., LEVRET, A., ALEXANDRE, P., LAMBERT, J. & VOGT, J., 1996. Historical seismicity of the Strait of Dover-Pas de Calais, *Terra Nova*, 8, 626-647.

REITER L., 1990, Earthquake Hazard Analysis, Columbia University Press, New York, 253 p.

VANDYCKE S., BERGERAT F. & DUPUIS F., 1988, Paleo-contraintes à la limite Crétacé-Tertiaire dans le Bassin de Mons (Belgique). Implications cinématiques. Relations avec la Zone de Cisaillement Nord-Artois, *C.R.Acad.Sci. Paris*, 307, 303-309.

VAN GILS, J.M., & ZACKEK Y., 1978. La séismicité de la Belgique et son application en génie parasismique. *Annales des Travaux Publics de Belgique*, 6, 1-38.

APPENDIX 1. The evaluation of seismic hazard: definition and methodology (from Ambraseys, 1983 and Reiter, 1990)

Definition of the seismic risk

The *seismic risk* is defined as the probability of the loss of property or lives within a given area and within a given period of time, resulting from earthquake-related natural phenomena.
On the other hand, the *seismic hazard* is the probability of occurrence of ground motion due to an earthquake of a particular magnitude, within a given area and within a given period of time.

The seismic risk (SR) and seismic hazard (SH) are linked by the following convolution equation:

$$SR = SH * VU * VA$$

where VA is the value of the elements exposed to the hazard and VU is their vulnerability.
If no lives or propriety exist, the risk is nil whatever the hazard is. On the other hand, in very urbanised areas, the risk could be significant even if the hazard is low to moderate. Vulnerability is the parameter that can be controlled by engineers to decrease the risk.

Computation of the seismic hazard

The seismic hazard is computed using a probabilistic approach which was first defined by Cornell (1968). In contrast to deterministic analysis, this approach allows to incorporate all the earthquakes believed to be able to generate a significant ground motion. The basic steps are the following:

Definition of earthquake source zones which can range from active faults to seismotectonic zones when earthquakes are not clearly linked to definite faults. A seismotectonic zone is a region of some geological, geophysical and seismological similarity that is assumed to possess uniform earthquake potential.

Characterisation of the activity within each earthquake source zone. Recurrence relationship, which indicates the chance of an earthquake of a given size to occur anywhere inside the zone during a specific period of time, is usually represented by the so-called Gutenberg-Richter law:

$$\log N = a - bM_S$$

where N is the cumulative number of events per year with magnitude equal to or larger than M_S, and a and b are two constants determined from the data set.

Determination of the attenuation laws suitable for the region, between a ground motion parameter (usually the peak horizontal acceleration) and the focal distance for earthquakes of different size. The attenuation laws are usually derived from strong-motion data recorded in a specific tectonic context.

Computation of seismic hazard maps which give the distribution of the peak acceleration for a given probability of non-exceedance during a given period of time. In the probabilistic approach, the seismic hazard at one given site is the sum of the contributions of all the earthquake sources.

Definition of the return period

Earthquakes are usually considered as random phenomena in space and time, following the Poisson distribution. The probability of exceedance of some level of ground motion during a time interval t is given by:

$$P(t) = 1 - \exp(-p_a t)$$

where p_a is the annual probability of exceedance. A very used parameter is the return period which is the reciprocal of p_a. Eurocode 8 requests to assess the seismic hazard for a 475 year return period, which corresponds to a probability of exceedance of 10% (or a probability of non-exceedance of 90%) in 50 years.

Manuscript received October 25, 1999 and accepted April 12, 2000.